I J R B A T, Issue (XIII) Volume (I) Jan 2025: 171-179
A Double-Blind Peer Reviewed & Refereed Journal
e-ISSN 2347 – 517X
Original Article
Reg. No. : MH-NGP/00001
INTERNATIONAL JOURNAL OF RESEARCHES IN BIOSCIENCES, AGRICULTURE AND TECHNOLOGY
© VMS RESEARCH FOUNDATION www.ijrbat.in

EFFECT OF CNT DOPING ON ENERGY BAND STRUCTURE OF HYDROTHERMALLY SYNTHESISED $Na_2Ti_6O_{13}$ PREPARED USING $Na_2Ti_3O_7$ AS AN INTERMEDIATE PHASE: A NOVEL APPROACH

Prashant Ambekar* & Jasmirkaur Randhawa#
*Department of Physics, Dharampeth M. P. Deo Memorial Science College, Nagpur -440033, INDIA
#Department of Applied Physics, Government College of Engineering, Nagpur- 441108, INDIA
pacific0701@gmail.com

Communicated :23.11.2024 | Revision: 26.11.2024 & 25.12.2024 Accepted: 31.12.2024 | Published: 30.01.2025

ABSTRACT:

In this paper, a novel approach of synthesizing $Na_2Ti_6O_{13}$ (NT) phase is reported. In the pristine intermediate phase, $Na_2Ti_3O_7$ (NT1) prepared by hydrothermal synthesis at 180^{o}C, CNTs are doped in the weight proportion of 0.1%, 0.3% and 0.5%. In the preparation process after adding and mixing the materials were annealed in Oxygen atmosphere. The pristine samples of both the phases and the doped samples were studied for structural characterization using XRD study and bandgap energies using UV-VIS spectra. Interesting results were obtained for the doped samples. The SEM did not show the presence of doped CNTs; however, the EDS showed a petite. The results show that the addition of CNTs in a small quantity change the overall band structure of the materials without leaving any trace of it in the host. A preliminary study is reported in this paper.

Keywords: - CNTs, Hydrothermal Synthesis, UV-VIS Spectroscopy, SEM and EDS, Band-Gap, etc.

INTRODUCTION:

Low-cost materials-based devices such as batteries, sensors, photovoltaic devices and many other are demanded worldwide (Liu, X., et al., 2020; Ambekar P. et al 2014, 2021; Randhawa J. et al, 2022). The energy demand is rising day by day due to rapid growth in use of handheld electronic gadgets and energy storage applications. So far, the whole world is dependent on Lithium based energy storages due its energy density and light weight (Ambekar P. et al, 2004). Most of the countries are fully or partially dependent on import of the Lithium based materials/devices as it is not abundantly available with them (Chu, S., et al. (2019). Moreover, the highly reactive nature of lithium when exposed to open air restricted its use in specific purposes. Looking at the shortcomings of the Lithium based devices; researchers are looking for the alternative materials to replace the lithium system fully or partially (Goodenough, J. B., et al., 2019). Sodium based materials are therefore preferred looking its less hazardous and cost-effective nature (Zhang, Y., et al., 2020).

Moreover, its versatility in fabricating devices is becoming more popular due to its suitability in many devices such as Open Reference Material for potentiometric type sensors, negative electrode for sodium-based batteries, tailor made ease in devising different form in simple nano processes (Zhang, Y., et al., 2020); Wang P. et al, 2020). In the recent literature, it has been seen that the synthesis techniques for ($Na_2Ti_3O_7$ and/or $Na_2Ti_6O_{13}$), hydrothermal synthesis is preferred by many researchers due to its simple and affordable type. Few recent papers and manuscripts were found of great use (Steven M. et al, 2017; Fagundes N. G. et al, 2019; Peiyuan Ji et al, 2019). So, started with a comparatively

http://doi.org/10.29369/ijrbat.2025.010.1.00012

simplest process given by Peiyuan Ji et al in his recently submitted manuscript to Nanotechnology. Wherein, he has emphasized on one dimensional layered or tunnel structure of battery electrodes for better energy storage device. Moreover, Zr and RuO_2 induced/impregnated $Na_2Ti_6O_{13}$ is studied by O. Vazquez-Cuchillo et al for water splitting application prove its versatility in different applications (Vazquez-Cuchillo O. et al, 2013).

Therefore, in current study, we have chosen to synthesis $Na_2Ti_6O_{13}$ by using hydrothermal method. The synthesized material is then used to prepare composite with CNTs in a weight ratio of 1:0.001, 1: 0.003 and 1:0.005, wherein the later are CNT percentages in pristine $Na_2Ti_3O_7$ phase. The synthesized composite materials along with pristine phases (Room temperature and at 500°C treated phases) then characterised by using XRD, SEM, EDS, UV-VIS spectroscopy.

MATERIALS AND METHODS:

Preparation of $Na_2Ti_3O_7$-$Na_2Ti_6O_{13}$:

The process followed as hydrothermal synthesis of $Na_2Ti_6O_{13}$ (NT2) via an intermediate phase $Na_2Ti_3O_7$ (NT1) at room temperature. The following steps were involved in the synthesis.

Drying the initial materials viz. TiO_2 with purity >99.98% (BDH brand) and NaOH with purity >98% (SRL Pvt. Ltd. India with assay >98%) at 110°C in the electric oven for overnight to evaporate the water contents present in it.

Weighing the materials in appropriate ratio (12 gm NaOH & 1gm TiO_2) using Mettler-Toledo mono-pan balance with accuracy 10-5 g.

Taken an appropriate quantity (30ml) of DI water in a cleaned and dried beaker and mixed the NaOH in it which then kept on a magnetic stirrer at 500 RPM rate at room temperature (28°C).

Added measured amount of powder of TiO_2 slowly and kept it running for ½ an hour.

The so obtained milky white material then placed in a hydrothermal bomb and kept it in an oven for about 24 hours at 180°C.

After cooling down it naturally to room temperature, a white precipitate is obtained which then washed with DI water multiple times (8-10 times) using centrifugal separation (REMI Centrifuge, C-24PLUS, Vasai, India) at 6000 RPM for 5 minutes and temperature of 15°C. Obtained material then dried at 90°C and sent for XRD and SEM characterization.

Preparation of Composites:

After characterization using XRD, the material is then mixed with CNT (CSIR- NPL synthesized) in the weight fraction ratios as (1NT1+0.001CNT), (1NT1+0.003CNT) and (1NT1+0.005CNT) hereafter referred as sample '1', '2' and '3' respectively (Hariharan K. and Maier J.,1995; Singh K. et al, 1999). The mixing process is done under DI water in a magnetic stirrer at room temperature at 500 RPM for 30 minutes each followed by 10 minutes ultra-sonication process. The steps involved in the process is given below-

Dried the prepared materials (room temperature phase) for 24 hours at 90°C.

The material was measured and made four batches each of 0.3 gm.

Keeping one aside three others were doped with CNTs procured from CSIR-NPL lab.

The composites were prepared as NT1: CNTs with already mentioned proportions.

The CNTs having very small amount and light in weight does not disperse under acetone even on ultra-sonication under DI water. Therefore, each composite was mixed manually using agate mortar and pestle for

http://doi.org/10.29369/ijrbat.2025.010.1.00012

about an hour each time after magnetic stirrer mixing at 500 RPM for 30 minutes.

The original material and three composites then placed in a tubular furnace with PID programming facility.

The rate of increment of temperature is adjusted as to reach 500°C in two hours. The temperature is maintained for another 3 hours and then cooled down naturally to room temperature.

All these annealing proceeded under constant O_2 flow to avoid possible contamination with other atmospheric gases and annealing under enriched O_2 so that during device performance no oxidation of CNT shall be allowed. The flow rate of O_2 is maintained minimal after purging it two times to remove traces of atmospheric gases present inside the tube of the furnace.

After annealing the samples gently crushed in to fine powder using mortar pestle under dry conditions.

The sample '0' (Annealed sample of Pure $Na_2Ti_6O_{13}$) is found a white fine powder as like the initial material before heat treatment, sample 'U80'. The composite samples '1','2' and '3' with CNT to 'U80' ratio 0.1%, 0.3% and 0.5% respectively were found as light grey, light grey-orange and light orange.

The pictures of all the five samples placed inside beakers in powder form are depicted in figure-1.

The so prepared 5 samples then characterized using XRD, SEM, EDS, UV-VIS characterizations.

Characterization Techniques:

a: X-RAY Diffraction:

The XRDs of all the five samples were characterized on a Rigaku Miniflex II DeskTop powder X-Ray Diffractometer using Cu-Kα wavelength with 2θ values ranging from 5 to 75 degrees having a step value of 0.02 degrees. A fine powder of each sample is provided for the measurement.

b: SEM and EDS:

The scanning electron microscopy and Energy-dispersive X-ray spectroscopy of all five powder samples were performed on Zeiss Evo MA10 Scanning Electron Microscope. The sample in powder form were mounted on a holder with carbon tape to stick the powder and then electrical contacts were made using silver paste at the sides and sputtered gold on the top of the sample to remove the electrons.

c: UV-VIS Spectroscopy:

The Ultraviolet-Visible light spectro-photometry is performed on Perkin Elmer Lambda-35 within 800-200 nm wavelength range. The samples were prepared in ethanol by dispersing a small quantity of the material using ultra-sonication. Before loading the sample in cubit, a reference ethanol data was taken to subtract from the actual data to minimise the error during entire experiment.

margins, apex acuminate. Panicles 10-22 cm long.

RESULT & DISCUSSION:

a: X-RAY Diffraction:

The powder XRD patterns of all the prepared materials are shown in figure-2. It has been very clear that the freshly prepared pristine phase NT1 (lowest in the graph) is altogether different than the other four and the phase is identified as $Na_2Ti_3O_7$. Wherein, most of the peaks' positions are matching with CAS number 72-0148 of the JCPDS data file. Moreover, no traces of precursors such as NaOH and TiO_2 were seen. As the sample is treated at 90°C for a whole day, it shows stability at room temperature keeping its structure and shape intact (monoclinic structure and rod shape in this case). The average particle

http://doi.org/10.29369/ijrbat.2025.010.1.00012

size of the materials using Debye-shearer's formula was found to be around 15.60 nm. After treatment at 500°C, the sample NT2 is completely changed and the phase identified as $Na_2Ti_6O_{13}$ as per the CAS Number 73-1398 of the JCPDS data file. However, the structure type (monoclinic) is not changed, but the peak positions changed drastically. Therefore, it is apparent that the phase NT1 is no longer stable at higher temperatures and gets converted in NT2 as depicted in figure-2.

The composites of NT2 with CNTs are however got little shifts in their peak positions towards higher angle side, however, it is small deviation. It is also seen that there is no extra peak seen in doped samples which proves there is no impurity phase available in CNT based composites.

b: SEM and EDS:

To observe the shape and sizes of the prepared materials at micro level Scanning Electron Microscopy (SEM) tool is used whereas to get the quantitative analysis of the materials, they are subjected to an Energy-dispersive X-ray spectroscopy (EDS) technique.

The SEM images of all samples show rod shapes in abundance sizing from 10s of nm to 100s of nm. Most of the nano-rods are seen coagulated and formed bundles of multiple rods. The details can be seen in the figure-3 (A, B, C, D & E). No CNTs were seen in the doped samples which shall be due to its low concentration and smaller size. However, all the diagrams show a porous structure consisting bundles and single rods, which indeed useful for battery electrode purposes.

The EDS analysis depicted in figure-4 shows that the pristine NT1 and NT2 does not show any % of CNTs whereas all other elements viz. Sodium, Oxygen and Titanium were seen. However, the composites show CNT less than 1% in embedded Na, Ti and O systems. This confirms that, even after annealing under oxygen atmosphere, certain CNT concentration is present in the NT2 system, which indeed tailored its performance under visible spectrum.

c: UV-VIS Spectroscopy:

Figure-5 clearly shows that most of the absorbance is observed in mostly in UV and partially in visible regions. Moreover, the samples NT1 is showing lower band gap as compared with the NT2. However, interestingly, the doped samples were showing lower band gaps as the % of CNT increases and are found as 2.81, 2.62 and 2.51 eV for 1NT2+0.001CNT, 1NT2+0.003CNT and 1NT2+0.005CNT respectively. This signifies the dopant, CNT has some surface phenomenon of reduction in band gap energy, which indeed find its use in device fabrication operating under visible region.

CONCLUSION:

The phase of prepared material using hydrothermal synthesis, $Na_2Ti_6O_{13}$ has been successfully produced via an intermediate phase, namely $Na_2Ti_3O_7$. Their structural characteristics with microstructure and grain size in the nano range were demonstrated by the XRD data with SEM and EDS. The final materials with CNTs added have different band gap energies, making them promising materials for use in devices. It has been discovered that the additional CNT phase changes the pristine NT2's characteristics and reduces its band gap, allowing for sideways electronic migration within the grain boundaries. Furthermore, since the EDS reveals no carbon traces, it might be a better choice for an appropriate Open Reference

http://doi.org/10.29369/ijrbat.2025.010.1.00012

Electrode material for potentiometric gas sensors.

FUTURE SCOPE:

In view of the device performance, precise optimization of the composite phase could be done and its impedance analysis can give better insight to the actual mechanism taking place when CNTs are added in to the pristine phase NT1 and annealed at 500ºC or higher temperatures. Precise measurements for visible range photo-conductance, Photo-luminescence and water splitting using these materials can be performed. Apart from these, the sensing response, a well optimised material, or a set of materials can be developed using the said materials and its synthesis procedure.

ACKNOWLEDGEMENT:

The author (PA) is thankful to the IAS, Bangalore; INSA, New Delhi and NASI, Allahabad for jointly awarding and sponsoring the Summer Research Fellowship awarded to him during Summer 2019 at the National Physical Laboratory, New Delhi and to the Supervisor, Dr. VidyaNand Singh for his guidance and laboratory facilities provided for the work.

REFERENCES:

Ambekar P, Randhawa J. and Singh K., (2014), Stabilizing the Sensing Electrode Kinetics of an Electrochemical CO_2 Gas Sensor Using Materials Engineering, Adv. Sci. Lett. 20 565-569.

Ambekar P. and Randhawa J., (2021), Surface Conductivity of Binary Carbonate as a Performance Governing Parameter of an Electrochemical CO_2 Gas Sensor, Bull. Mater. Sci. 44:235 https://doi.org/ 10.1007/s12034-021-02526-y.

Ambekar P., Randhawa J., and Singh, K., (2022), Charge transfer mechanism in $KNbO_3$ dispersed composites of monovalent alkali carbonate, Ferroelectrics; 587:1, 84-94, DOI: 10.1080/00150193.2022.2034418 .

Ambekar P., Randhawa J., Bhoga S. S., and Singh K., (2004) Galvanic CO_2 sensor with Li_2O: B_2O_3 glass ceramics-based composite, Ionics 10, 45-49

Chu, S., et al. (2019). "Low-cost energy storage and conversion devices: Opportunities and challenges." Energy & Environmental Science, 12(11), 3311-3324. doi: 10.1039/C9EE02431K

Goodenough, J. B., et al. (2019). Beyond Lithium: Alternative Materials for Energy Storage. Chemical Reviews, 119(10), 5718-5746.

Hariharan K. and Maier J. (1995), Enhancement of the fluoride vacancy conduction in PbF_2: SiO_2 and PbF_2: Al_2O_3 composites, J. Electrochem. Soc. 142 3469.

Liu, X., et al. (2020). "Low-cost materials for energy storage and conversion." Materials Today, 33, 34-44. doi: 10.1016/j.mattod.2020.02.003

Fagundes N. G. et al, Solid State Sciences, Volume 88, February 2019, Pages 63-66, https://doi.org/10.1016/j.solidstatesciences.2018.11.014

Peiyuan Ji et al, (2019); In-situ Growth of MnO@$Na_2Ti_6O_{13}$ heterojunction nanowires for high performance supercapacitors, Nanotechnology 30(33), https://doi.org/10.1088/1361-

http://doi.org/10.29369/ijrbat.2025.010.1.00012

6528/ab0cd1

Randhawa J. et al, (2022), Low-Cost Lithium Carbonate- Silica Gel Electrolyte System for Electrochemical Device Application, RTMNU Science Journal, vol. XV, pp.1-6.

Scherrer P. (1918), *Gottinger Nachrichten Gecell.* Mathematisch-Physikalische Klasse, 2 98.

Steven M., Girish M. Kale, Electrochimica Acta Volume 258, 20 December 2017, Pages 1059-1063, https://doi.org/10.1016/j.electacta.2017.11.158

Vazquez-Cuchillo O. et al, Journal of Photochemistry and Photobiology A: Chemistry, 266 (2013) 6-11.DOI:10.1021/acs.analchem.8b04681

Wang, P., et al. (2020). Sodium-based materials for energy storage and sensing applications. Journal of Materials Chemistry A, 8(15), 7341-7355.

Zhang, Y., et al. (2020). Nanostructured sodium-based materials for energy storage and conversion. ACS Applied Materials & Interfaces, 12(2), 2531-2546.

Zhang, Y., et al. (2020). Sodium-based anode materials for sodium-ion batteries: A review. Journal of Materials Chemistry A, 8(15), 7341-7355.

Figure:1. Annealed samples at 500°C showing different colors- NT1(white), NT2(white), 1(light gray), 2(light gray-orange) and 3(light orange)

http://doi.org/10.29369/ijrbat.2025.010.1.00012

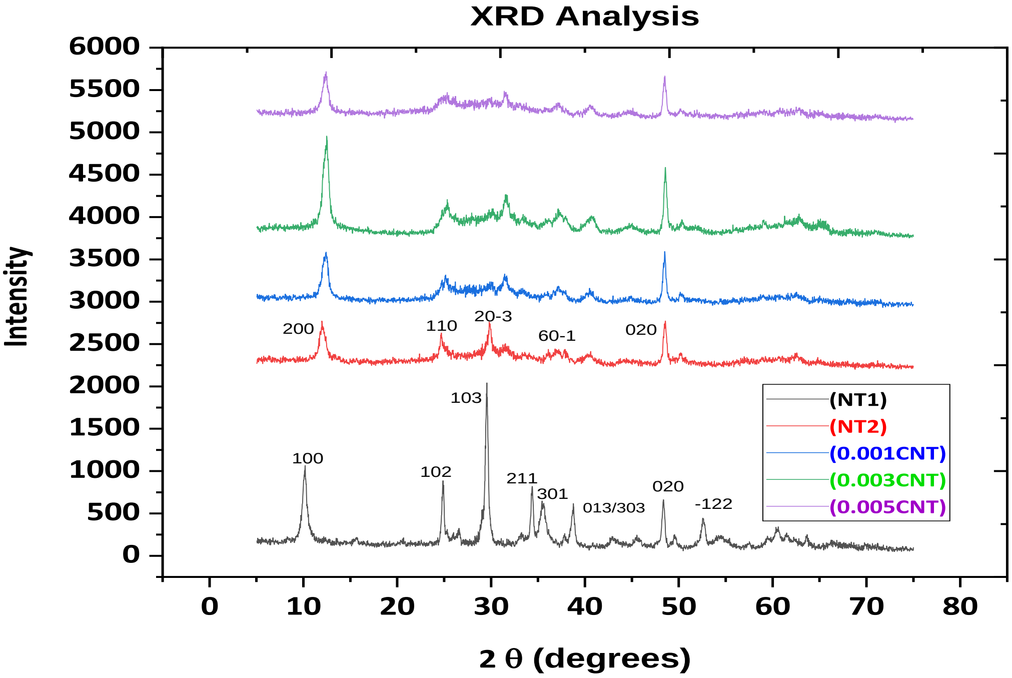

Figure- 2: X-ray diffraction patterns of all the prepared samples and their comparison is depicted

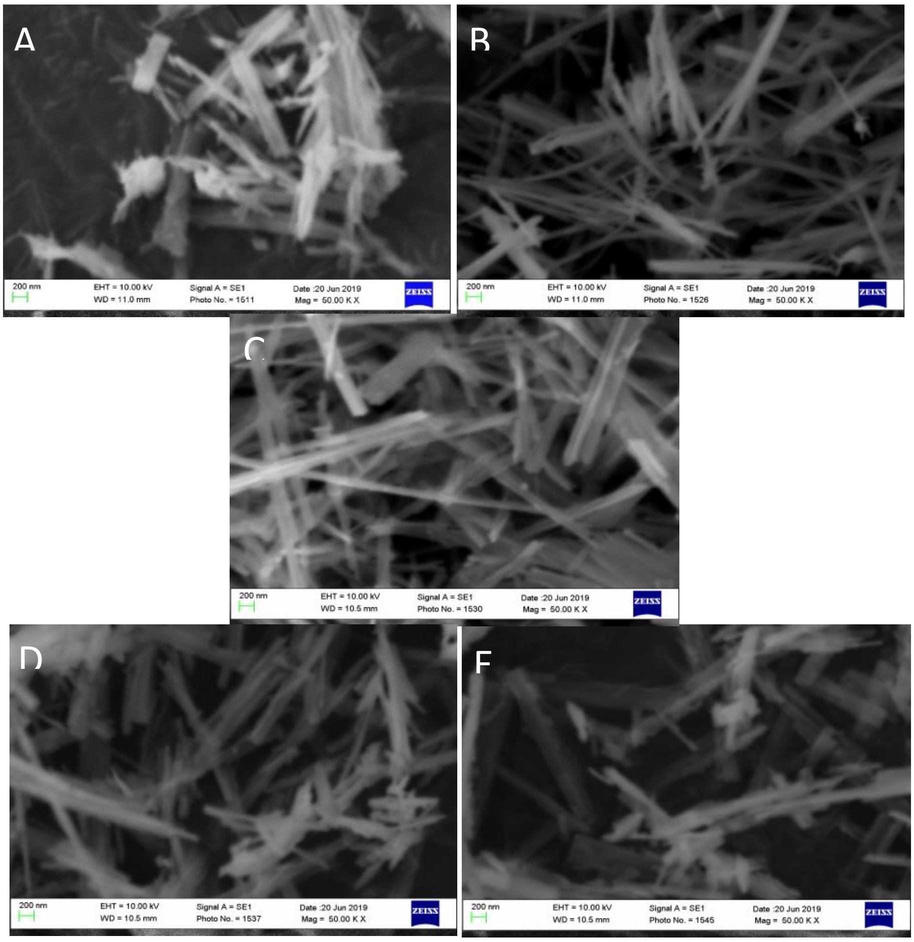

Figure-3: SEM image for NT1, NT2, NT2+0.001 CNT, NT2+0.003CNT and NT2+0.005CNT are depicted in figure A, B, C, D and E respectively.

http://doi.org/10.29369/ijrbat.2025.010.1.00012

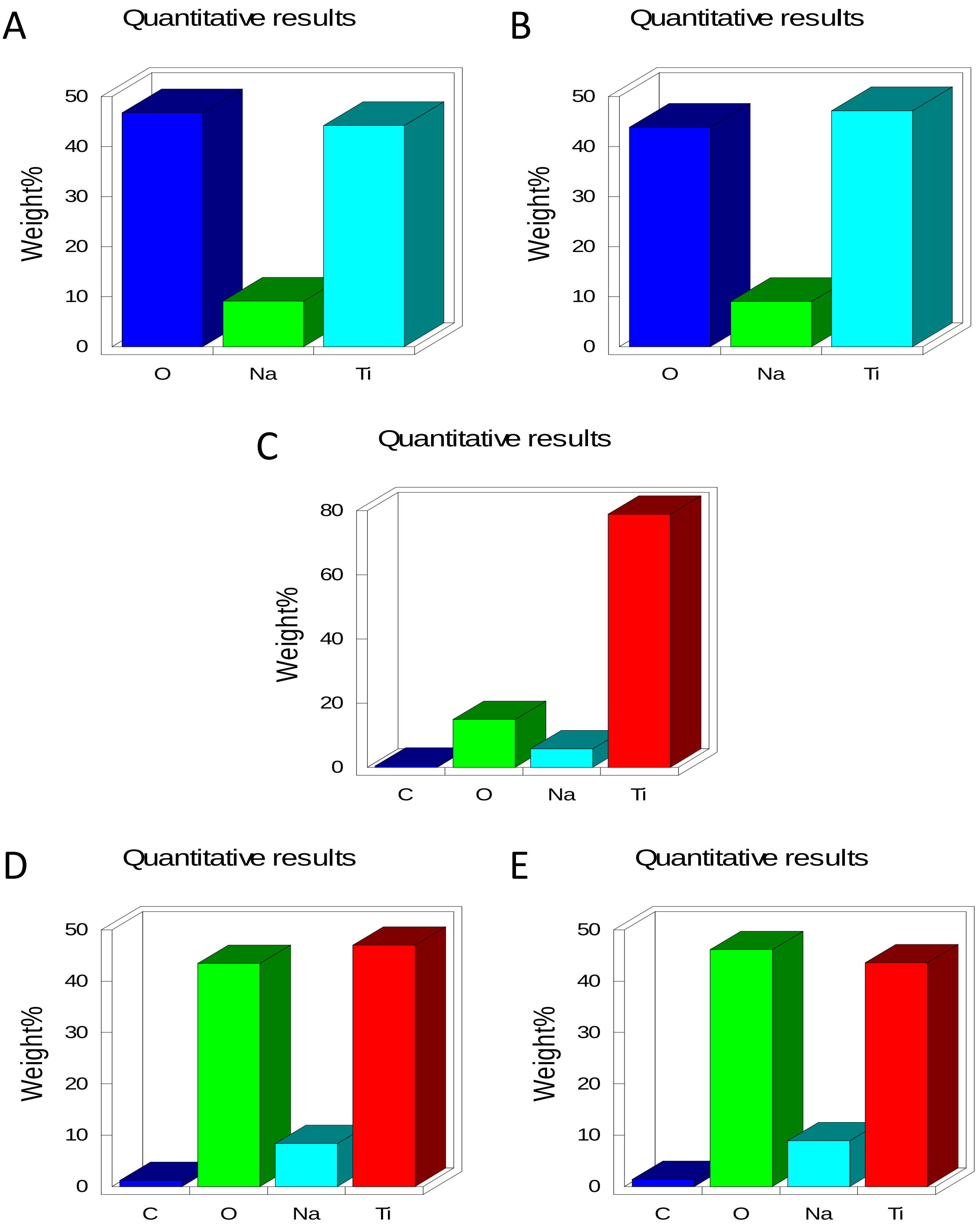

Figure-4: EDS bar diagrams showing quantitative analysis for NT1, NT2, NT2+0.001 CNT, NT2+0.003CNT and NT2+0.005CNT are depicted in figure A, B, C, D and E respectively.

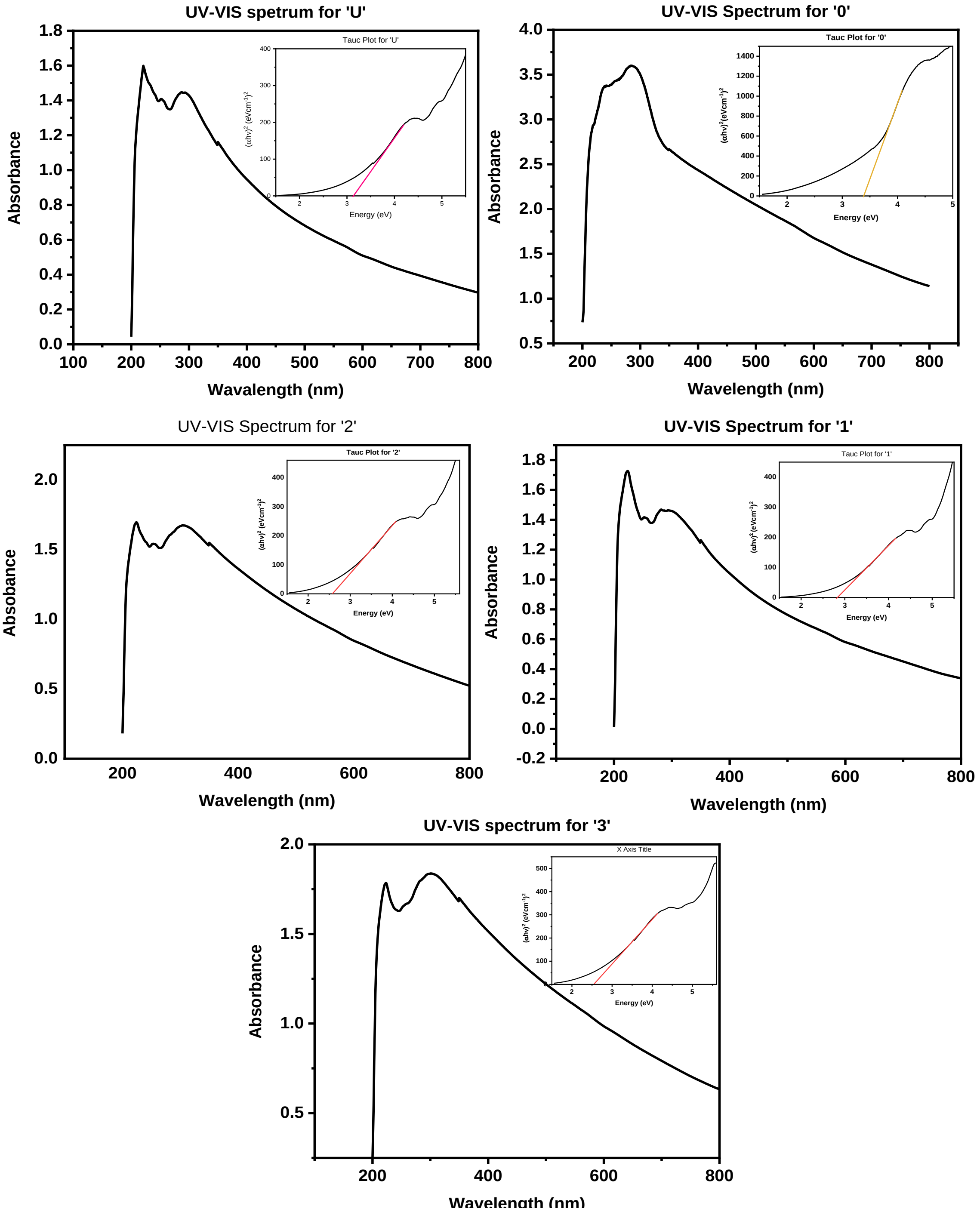

Figure-5: Wavelength dependent absorbance for NT1, NT2, NT2+0.001CNT, NT2+0.003CNT and NT2+0.005CNT are depicted in figure U, 0, 1, 2 and 3 respectively. The Band gap for each sample is seen in the insets.